On the Mechanism of NO Selective Catalytic Reduction by Hydrocarbons over Cu-ZSM-5 via X-ray Absorption Spectroscopic Study

Di-Jia Liu*

AlliedSignal Incorporated, 50 East Algonquin Road, Des Plaines, Illinois 60017-5016

Heinz J. Robota

ASEC, P.O. Box 580970, Tulsa, Oklahoma 74158-0970

Received: September 17, 1998; In Final Form: January 11, 1999

An understanding of the catalytic mechanism of NO_x reduction is critical for the development of next-generation high-fuel efficiency, low-emission vehicles. This paper compiles our investigations in recent years on the mechanism of NO selective catalytic reduction (SCR) by hydrocarbon over Cu-ZSM-5. The studies were focused on the oxidation state and coordination chemistry of the exchanged Cu as the active site during the catalytic reaction using X-ray absorption spectroscopic (XAS) techniques, mainly XANES and EXAFS. Our experiment demonstrated the existence of a redox mechanism which involves cyclic switching of the oxidation states between Cu(II) and Cu(I) in an oxygen-rich gas mixture under elevated temperature. We also observed the coordination structural change of copper ion in ZSM-5 accompanying the change of oxidation state. A correlation between cuprous ion concentration and catalytic activity was found in NO SCR by propene. The impact of another two hydrocarbons, propane and methane, on the copper redox behavior also appears to correlate to catalytic activities in the respective mixtures. Discussions on the nature of the active sites and the mechanism of SCR are presented based on the XAS data analysis. The similarity and difference of the physical properties of copper ion between NO catalytic decomposition and NO SCR are also discussed.

Introduction

The catalytic activity of Cu-ZSM-5 toward NO decomposition and NO selective catalytic reduction (SCR) with hydrocarbons has been investigated over the past 8 years.[1,2] Although the poor hydrothermal stability seems to hamper its practical applications, Cu-ZSM-5 has been extensively studied as a "model system". Consequently, it has led to the discovery of a series of zeolite-based transition-metal NO_x abatement catalysts. A wealth of information has been cumulated through kinetics, physical characterization, and theoretical studies[3−17] and was reviewed recently.[18] To complement the existing characterization methods, our investigation using the X-ray absorption spectroscopic technique has been focused on two important aspects of this catalyst system, i.e., the nature of the active site and the behavior of the active site under reaction condition. It is our hope that this information will provide additional, in-depth understanding on the physical and chemical processes in the NO_x reduction catalytic system and facilitate development toward a more practical NO_x reduction catalyst.

The in situ X-ray absorption spectroscopic techniques used in this study are XANES and EXAFS. We have demonstrated that both techniques are very versatile in investigating the catalyst properties of copper-exchanged zeolite during direct NO decomposition and SCR by hydrocarbons.[19−21] While the mechanism of direct NO decomposition has been discussed in detail in our earlier reports,[19,20] this paper focuses mainly on the following issues about NO SCR by hydrocarbons: (a) Could the redox chemistry involving the switching of oxidation states between cupric Cu(II) and cuprous Cu(I) exist in a highly oxidative environment of NO SCR? (b) If it could, does Cu(I) formation follow the same route as that in the direct decomposition case? (c) What are the electronic and coordination structural properties of the active site, and how they are influenced by the reaction conditions? (d) How do different types of hydrocarbons impact the nature of the active site? (e) What is the role of oxygen in NO SCR? Our approach to these questions is to establish as much experimental evidence as we can with the catalytic environment as close to the real operating conditions as possible.

The X-ray absorption near-edge structure (XANES) method utilizes the absorption features of a specific atomic core transition near the threshold of the energy continuum which directly relates to the electronic configuration and the stereochemistry. Because of the nature of the electronic transition to the highly excited, quasi-stable Rydberg states, narrow features often occur near the edge jump in the XANES spectrum which are very useful in characterizing the population at a specific oxidation state. These features work particularly well in distinguishing the cupric and cuprous ions coexisting in Cu-ZSM-5. For example, Cu(I) has a d^{10} closed-shell electronic configuration; therefore, it cannot be directly probed by some conventional analytical method such as ESR. In the X-ray absorption spectra, the Cu(I) $1s \rightarrow 4p_{x,y}$ electronic transition appears as a sharp, intense peak between 3 and 5 eV above the threshold (E_0) of the Cu^0 transition. This peak is clearly separated from the corresponding Cu(II) transition, which appears in the 7−9 eV range. The subtle energy shift defines the change of chemical environment and variation of the transition intensity translates to the change of the population. These features were used extensively in characterizing the nature of the copper ions under dynamic catalytic reaction condition in this study.

10.1021/jp983761l CCC: $18.00
Published on Web 03/20/1999

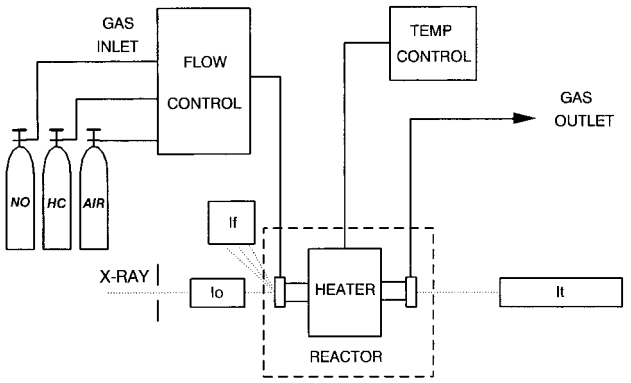

Figure 1. Schematic diagram of the in situ reactor system for X-ray absorption spectroscopic studies during catalytic reduction of NO by hydrocarbons.

Extended X-ray absorption fine structure (EXAFS) spans a broader energy region well above the threshold in the X-ray absorption spectrum. The coordination shell structure of the selected atom can often be obtained through the Fourier transformation of the resonance feature in the energy or wave vector space, i. e., the χ function. In this study, EXAFS is used mainly to characterize the coordination chemistry of the atomically dispersed copper ions under the in situ condition.

The combination of XANES and EXAFS offers an excellent tool to study the electronic and geometric structural changes in a catalyst simultaneously. Cu-ZSM-5, in retrospect, is almost uniquely suited for these XAS techniques because of the high degree of copper dispersion. The XAS techniques directly reveal the nature of the transition-metal active site, which compliments other techniques of probing the site through the study of the adsorbate, such as FTIR. Another major advantage of EXAFS and XANES is their nonintrusiveness. Because the X-ray can penetrate the catalyst samples without interfering with the catalytic process, it is feasible to design an experiment to study the catalyst behavior under *true* reaction temperature and pressure. This is critically important in Cu-ZSM-5 study, as we will demonstrate in this report.

Experimental Section

Catalyst Preparation. The Cu-ZSM-5 samples in this study were made by exposing commercial H-ZSM-5 materials (typically with Si/Al atom ratios of 30) to aqueous cupric acetate solution. The details of the Cu exchange procedure are given in ref 22. This procedure can result in incorporation of cupric ions greater than the nominal exchange capacity of the zeolite. We define a sample's name based on its exchanged level. For example, a Cu-ZSM-5-150 catalyst contains a cupric ion content of 150% of the nominal exchange capacity of the zeolite which, equivalently, contains a Cu/Al atom ratio of 0.75. The samples studied in this experiment are calcined in dry air at 673 K for 2 h after ion exchange and filtration. No further aging process was involved.

In Situ X-ray Absorption Spectroscopy Experimental Setup. To characterize copper in Cu-ZSM-5 during catalysis, we designed an in situ reactor system with which we can perform NO SCR under a real catalytic reaction while taking X-ray absorption spectra. Shown in Figure 1 is the schematic diagram of the reactor system. The reactor consists of a heater and a tube reactor where the NO reduction reaction occurs at the midsection. About 70 mg of 150% ion-exchanged Cu-ZSM-5 is loosely packed as a thin, permeable disk 1 cm in diameter and placed in a sample holder at the center of the tube reactor. The reactor is heated by the insulated resistive heater. The sample weight was adjusted according to the copper loading in the zeolite so as to achieve the optimal X-ray absorptivity, $\mu x = 2$, where μ is the overall absorption coefficient of the catalyst and x is the sample thickness. The sample holder was designed in such a way that all the reactant flow must pass through the catalyst, similar to a "plug-flow" reactor. A well collimated X-ray beam passed through the X-ray intensity calibrator I_0 and the sample holder and entered the transmission detector I_t where the absorption of X-rays was recorded. At the entrance of the reactor, a small piece of Cu foil on a Pb plate was placed to partially block the incident X-rays for energy calibration. The actual horizontal beam width passing catalyst sample inside was 8 mm. The fluorescence excitation spectrum of Cu foil outside of the reactor was collected simultaneously by a detector I_f during each scan to calibrate the Cu^0 edge energy. The zero of energy in this experiment is defined as the first inflection point of the copper metal.

The copper ion state-to-state transition energy is a critical parameter for this experiment. The measurement accuracy is typically limited to about ± 0.2 eV due to the monochromator resolution. Furthermore, the incident angle between the X-ray and Cu foil often varies between each experiment which results in a slight shift of the reference. To appropriately correct these instrument factors, we also calibrate the X-ray energy by remeasuring the narrow $1s \rightarrow 4p$ transition of Cu(I) formed through oxygen desorption from the same Cu-ZSM-5 sample at the beginning of each experiment.

The X-ray absorption experiment reported in this investigation was performed at Beamline X-18B of the National Synchrotron Light Source (NSLS), Brookhaven National Laboratory. The synchrotron ring current during this experiment was in the range 110−210 mA, and the ring energy was 2.53 GeV. A pair of Si(220) crystals was used in the monochromator, and the slit width of the monochromator exit was 0.2 mm vertical and 15 mm horizontal to ensure optimal resolution. All the near-edge X-ray absorption spectra were taken at the Cu K-edge (8979 eV) with energy resolution better than 0.5 eV. For the EXAFS experiment, a typical spectrum covers a wave vector, k, range of 14 $Å^{-1}$ for an appropriate Fourier transformation.

This reactor system is a simplified version of that used in the NO decomposition study which we reported earlier.[19,20] In addition to 1%NO/N_2, dry air, and high-purity He used in the NO decomposition study, 1% C_3H_6/N_2, 1% C_3H_8/N_2, and 1% CH_4/N_2 (all by Matheson) are also used in this study. The flow of each reactant is calibrated by an electronic flow controller, and the concentration of the mixture is adjusted to the desired level. The total flow rate is regulated so that the space velocity across the catalyst bed ranges from 80 000 to 120 000 GHSV. During in situ measurement, the temperature of the reactor is adjusted from room temperature up to 873 K. Because of the excess oxygen used in the experiment, the NO conversion monitoring scheme used in our NO decomposition study is no longer adequate.[19] Therefore, no NO conversion is measured on line.

Plug-Flow Reactor for in Situ X-ray Absorption Study. Another challenge for in situ X-ray absorption measurement is the limit of catalyst sample quantity due to the X-ray penetration depth. To achieve a maximum signal-to-noise ratio, the amount of sample often has to be limited to a rather small quantity, such as in this study. The reactor design, therefore, has to ensure an effective catalytic conversion to produce a sufficient amount of product to be monitored simultaneously. The reactor also has to sustain repeated high-temperature stress. Although we

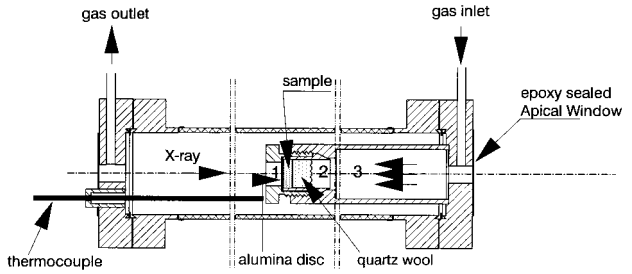

Figure 2. Design diagram of the "plug-flow" reactor for in situ X-ray absorption spectroscopic study.

did not monitor the effluent in this study, we used the same plug-flow reactor from our earlier NO decomposition study. In that study, the reactor was shown to be effective in meeting the above requirements.

Shown in Figure 2 is the reactor design. Basically, a stainless steel AN-type female connector from Swagelok was modified and welded onto a stainless steel inlet tube (o.d. = 0.85 in.) from which the flow of the reactant mixture enters (Part 3 in Figure 2). The removable sample holder consists of two parts. The center part is a tubular stainless steel holder with a male AN-type head (Part 2). This central tubular holder is held by an outer tube with matching thread to the flow tube (Part 1). A very small (0.002 in.) gap is left between the center and outer tubes where a thin alumina filter membrane disk with a >60% opening of straight channels is placed. During the experiment, a layer of catalyst powder with a particle size less than 100 mesh is packed into the center tube holder. The function of the alumina membrane disk is to physically hold the sample powder at the downstream side while allowing the reactant flow through with minimum resistance. At the upstream side, a small amount of quartz wool is inserted to support the powder. The whole assembly is fastened onto the female AN connector at the end of the flow tube. The flow tube assembly is enclosed in the center of a quartz tube (o.d. = 1.5 in., length = 15 in.) of which the catalyst section is surrounded by a resistive heating unit. At each end of the tube, the X-ray transparent window made of 25 μm thick apical film was epoxy-sealed. Using a metal-to-metal AN-type connection, we were able to seal the junction between the in-flow tube and the sample holder in order to force the gas through the catalyst bed without bypass. The stainless steel construction is relatively corrosion free and thermally stable during repeated temperature treatment up to 873 K. The relatively large opening of the sample holder (d = 10 mm) allows us to pack a thin layer of catalyst, which is sufficient to produce detectable amounts of products from the reaction. The uniformity of the thin layer is also ideal for X-ray absorption spectroscopy. During the reaction, the sample temperature is probed by a thermocouple of the temperature control unit. The tip of the thermocouple contacts closely to the sample holder. Another advantage of this reactor design is the long, stainless steel inlet tube (16 cm). As part of the reactor, the inlet tube connects directly with the sample holder and is heated by the tubular furnace simultaneously. In this configuration, the gas is preheated before it reaches the catalyst sample. Therefore, the temperature reading on the control unit accurately reflects the true catalysis temperature.

Although the reactor furnace can reach as high as 1300 K, two factors restrict the upper limit of the present reactor design: (a) the stainless steel sample holder cannot be heated much above 973 K, (b) the alumina disk undergoes phase transition and disintegrates around 1000 K. Both limitations can be lifted by replacing these parts with high-temperature performance materials.

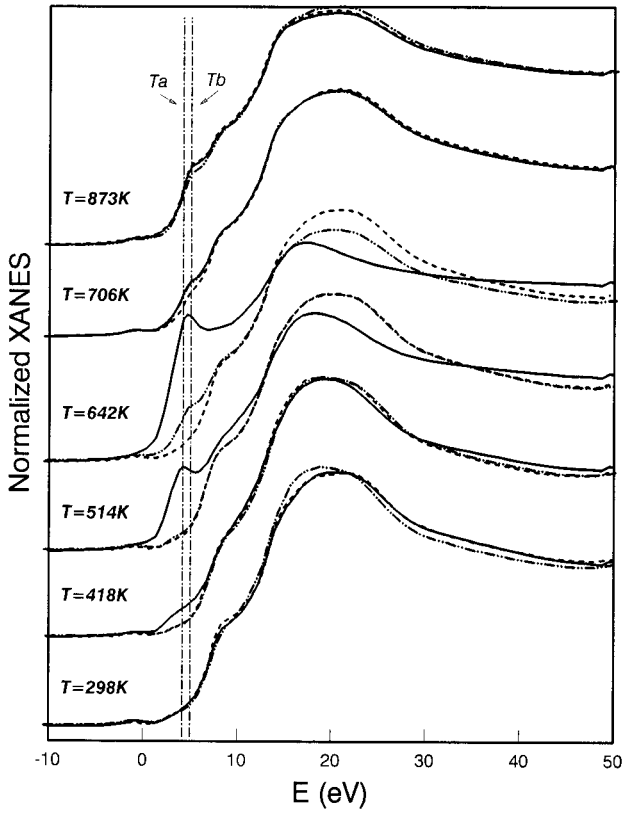

Figure 3. XANES spectra of Cu in Cu-ZSM-5 at different temperatures in the reactant mixtures containing $NO/C_3H_6/O_2/N_2$ = 3200vppm/3200vppm/7.5 vol %/balance (—); $NO/C_3H_8/O_2/N_2$ = 3200vppm/3200vppm/7.5 vol %/balance (- · -); and $NO/CH_4/O_2/N_2$ = 2300vppm/5200vppm/5.3 vol %/balance (- - -).

Observations

Temperature Dependence of Cu(I) Intensity versus SCR-C_3H_6 Activity. The NO SCR with hydrocarbons is highly temperature dependent. The optimal NO conversion to N_2 over Cu-ZSM-5 usually occurs around 625 K, which is about 150 K lower than that of direct NO decomposition reaction. To understand how the Cu oxidation state and coordination chemistry is related to the catalytic activity, we first investigated the changes in the Cu XANES spectrum of Cu-ZSM-5 by increasing the reaction temperature incrementally across the optimum NO conversion temperature. To minimize the potential interference by any residual hydrocarbons left on the catalyst surface, the catalyst was first calcined in situ in flowing dry air at 773 K for 1 h in order for it to be fully oxidized and dehydrated. The reactor temperature was then ramped up at 5 K/min from room temperature to 873 K in a gas mixture of $NO/C_3H_6/O_2$ = 3200vppm/3200vppm/7.5 vol %, balanced by N_2. A series of XANES spectra were taken at 30° intervals during the linear increase in reaction temperature. We observed that even with excess oxygen in the stream, a significant fraction of the copper ions in ZSM-5 is gradually reduced to Cu(I) at elevated temperature. Shown by the solid line in Figure 3 are a selected group of XANES spectra taken during the temperature rise. XANES spectra show that a narrow peak starts to appear near the X-ray absorption threshold energy with the increase of the catalytic temperature. The intensity of this transition increases gradually when the reaction temperature reaches about 500 K and decreases abruptly when the temperature is above

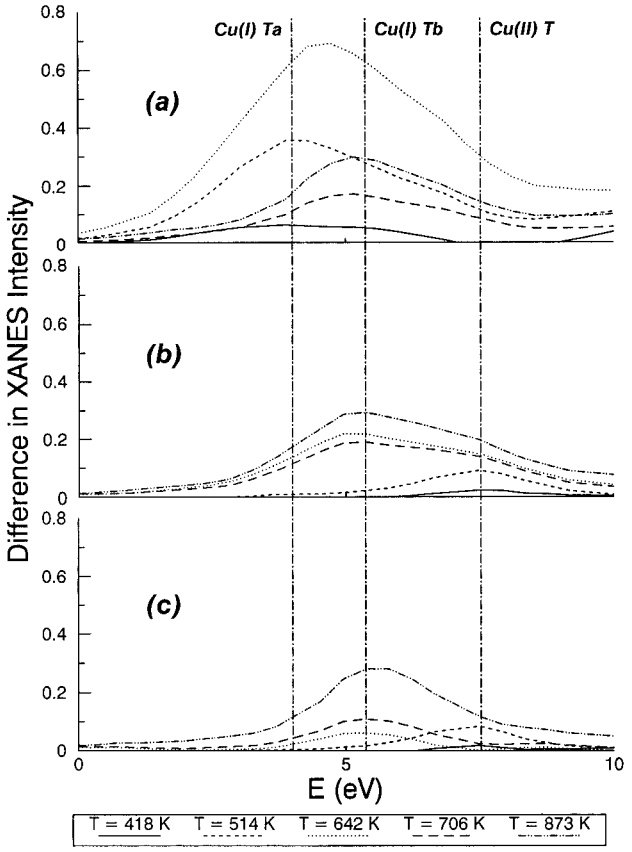

Figure 4. Normalized difference XANES spectra of Cu in Cu-ZSM-5 at different temperatures in the reactant mixtures containing (a) NO/C_3H_6/O_2/N_2 = 3200vppm/3200vppm/7.5 vol %/balance; (b) NO/C_3H_8/O_2/N_2 = 3200vppm/3200vppm/7.5 vol %/balance; and (c) NO/CH_4/O_2/N_2 = 2300vppm/5200vppm/5.3 vol %/balance.

670 K. This peak was assigned to the Cu(I) 1s → 4p transition from previous studies on cuprous compounds.[19,23] Accompanying the variation of peak intensity, the peak center also shifts gradually from 4 eV (marked by the first vertical dashed line) to a higher energy. At temperatures above 670 K, the peak appears 1.3 eV higher (marked by the second vertical dashed line at $E = 5.3$ eV) with a much weaker transition intensity. Further increase of the reactor temperature results in the increase of Cu(I) peak intensity, while the peak energy remains unchanged.

To emphasize the change of the Cu(I) 1s → 4p transition between 0 and 10 eV, we also plotted the normalized difference XANES spectra, shown in Figure 4a. These spectra were obtained by subtracting XANES at different temperatures in Figure 3 from that at room temperature.[19,23] After integrating the Cu(I) 1s → 4p peak area for the normalized difference XANES spectra for all the experimental points, we obtained the change in the Cu(I) transition intensity with the reaction temperature. They are plotted as the solid circles in Figure 5. The integrated Cu(I) transition intensity is proportional to the cuprous ion concentration based on the first-order estimate. It is also consistent with the result from another XANES spectral fitting method.[19,20] In the reaction mixture of NO/C_3H_6/O_2/N_2 there clearly exists a window of enhanced cuprous ion concentration from 500 to 700 K, which peaks at about 640 K on a continually rising background.

We also plot, solid line in Figure 5, the NO conversion level to N_2 in selective reduction by propene reported by Iwamoto and co-workers.[3] In this figure the NO conversion level as well as the relative Cu(I) concentration we observed are both

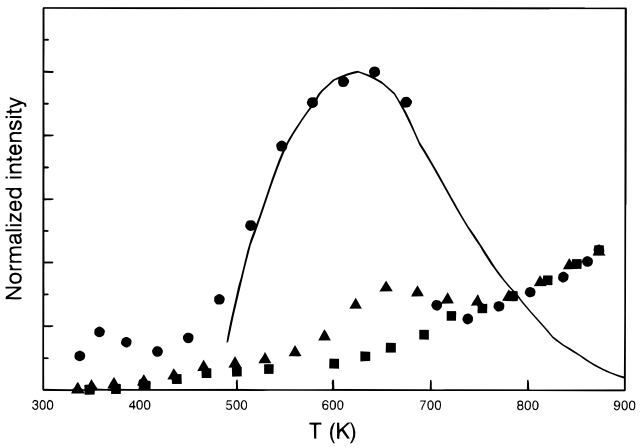

Figure 5. Normalized concentration of Cu(I) at different temperatures in the reactant streams of NO/C_3H_6/O_2/N_2 = 3200vppm/3200vppm/7.5 vol %/balance (●); NO/C_3H_8/O_2/N_2 = 3200vppm/3200vppm/7.5 vol %/balance (▲); and NO/CH_4/O_2/N_2 = 2300vppm/5200vppm/5.3 vol %/balance (■). To compare with the catalysis result, the NO conversion level to N_2 measured by Iwamoto and co-workers[3] (normalized at the peak value) is also plotted (—).

normalized to their respective peak values. They match very well in the temperature range between 500 and 700 K. Above 700 K, however, a considerable discrepancy was observed between the two. Considering the variation of the conditions between the two experiments, such as gas composition, flow rate, different reactor, etc., the excellent match between 500 and 700 K also could be accidental. However, a similar temperature window for selective NO reduction was observed by other groups[6,10,22] at different conditions, although the actual conversion temperatures may be shifted slightly.

The window of Cu(I) enhancement between 500 and 700 K is relatively insensitive to the amount of propene in the stream within certain limits. For example, we observed an almost identical Cu(I) intensity profile when propene concentration was decreased to 1000 ppm in the reaction gas mixture of NO/C_3H_6/O_2/N_2 = 1000vppm/1000vppm/2.0 vol %/balance.

We should point out that a similar temperature dependence of Cu(I) concentration was also observed during the *decrease* of the reaction temperature, except that the window shifted to slightly lower temperature by about 50 K. Unless the catalyst has been operated at low temperature for a substantial amount of time and during which period severe coking was formed, the amount of Cu(I) content observed at room temperature after cooling is usually very low. Cu(I) is nearly completely reoxidized to Cu(II) upon cooling. This observation further demonstrated that the state of the active site observed at the optimum reaction temperature is generally very different from that observed at the "static state" after catalysis. It is impossible to "freeze" the active site at catalytic temperature and study it at room temperature. Therefore, it is imperative to monitor the catalyst's state in situ in the dynamic environment.

Coordination of Copper Ions during Catalysis. Corresponding to the change in the copper oxidation state, we also observed the change of the number of oxygen ligands surrounding the copper ions. This structural information was obtained through the analysis of EXAFS spectra recorded under in situ conditions. Shown in Figure 6 are three radial distribution functions (RDF) of Cu in Cu-ZSM-5−150 derived from direct Fourier transformation of EXAFS spectra. The EXAFS spectra were obtained at three different stages of SCR of NO by propene during the temperature ramp. They represent the conditions (a) at room temperature immediately after the catalyst was oxidized

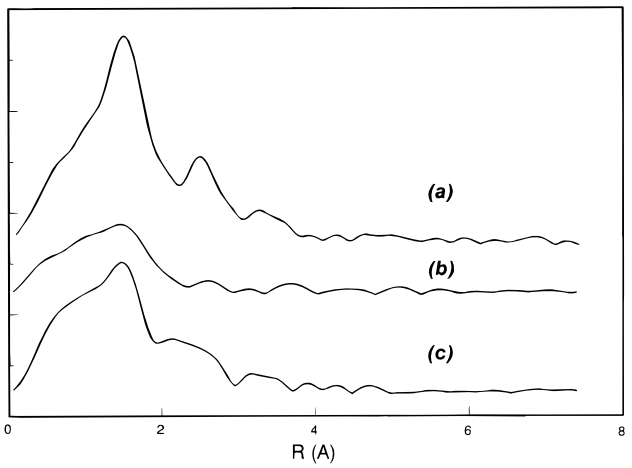

Figure 6. Radial distribution functions (RDF) of Cu in Cu-ZSM-5-150 obtained from Fourier transformation of the EXAFS χ functions. The EXAFS spectra were taken at three stages of SCR of NO by propene during a temperature ramp: (a) at room temperature immediately after the catalyst was oxidized by dry air, (b) at optimum NO conversion temperature (674 K) in the $NO/C_3H_6/O_2/N_2$ reaction mixture, and (c) at 823 K in the reaction mixture.

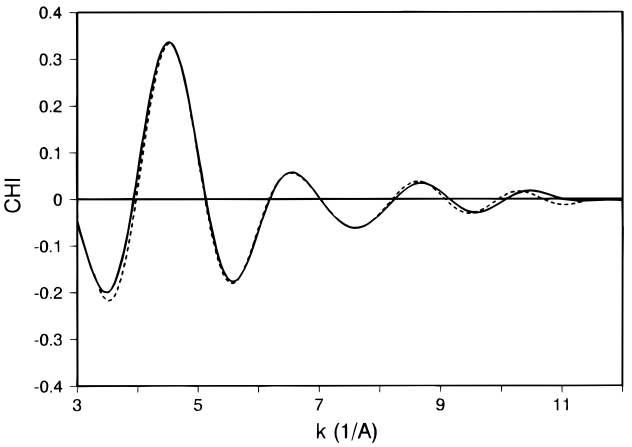

Figure 7. χ functions of the first-shell O surrounding Cu after the Cu-ZSM-5−150 is oxidized by dry air: (—) filtered experimental data (- - -) nonlinear least-squares fitted data.

and dehydrated by dry air, (b) at optimum NO conversion temperature (625 K) in the $NO/C_3H_6/O_2/N_2$ reaction mixture and (c) at 823 K in the reaction mixture. Using a standard method of the nonlinear least-squares fitting to the inverse Fourier-transformed EXAFS functions, we derived the first-shell structure of the oxygen ligand surrounding the copper ions in Cu-ZSM-5. The fitting of the first shell is excellent, as demonstrated in Figure 7. We did not include the result of higher shell fitting in this study. Even though the higher shell structure is very valuable in defining the Cu ion location within the zeolite, we do not feel that the fitting is unambiguous at present, especially under the reaction conditions, due to the interference from large amplitude thermal motion at the elevated temperature. The structural parameters for the first coordination shell under all three reaction conditions are listed in Table 1 where N, R, and $\delta\sigma^2$ represent the number of the coordination, shell radius (or bond length), and difference of the Debye−Waller constant from that of the reference, respectively. A highly dispersed CuO/SiO_2 (1.6 wt % copper loading) was used as a reference compound from which the standard Cu−O phase and amplitude functions are extracted. Our earlier experiment showed that in dry air flow, the cupric ion in CuO/SiO_2 maintains four oxygen coordination and has a stable first-shell structure.

TABLE 1: First-Shell Coordination Number *N* and Shell Radius *R* of Cu-ZSM-5-150 at Different Stages of NO SCR by Propene

	N	R (Å)	$\delta\sigma^2$ (Å^2)
$T = 298$ K, after calcination in air	3.6	1.93	0.0002
$T = 625$ K, in $NO/C_3H_6/O_2/N_2$ mixture.	2.1	1.94	0.004
$T = 823$ K, in $NO/C_3H_6/O_2/N_2$ mixture.	3.4	1.93	0.001

Immediately after dehydration in dry air, copper in Cu-ZSM-5 is fully oxidized and coordinated by approximately four oxygen atoms. The RDF in Figure 6 also clearly shows the second and higher shell structures, presumably due to the backscattering from Si and O in the zeolite framework. The detailed discussion on the local structure after air oxidation has been given by our earlier study.[20] At the optimum NO conversion temperature, the 1s → 4p transition intensity of cuprous ion reached its peak while the average O coordination number decreased to about two. Although the bond distance of Cu−O is barely changed, the breadth of the Cu−O radial distribution increases significantly. In fact, this change is also reflected by the increase of the difference in the Debye−Waller constant listed in Table 1. The broader peak suggests (a) a less-rigidly bonded Cu−O which vibrates with higher amplitude and (b) coexistence of two or more types of copper−oxygen interactions or backscattering from another low atomic number atom, possibly carbon, from a similar bond distance. A further increase of the reaction temperature to 823 K prompts the drastic reoxidation of Cu(I) to Cu(II). Meanwhile, the oxygen coordination number is restored, although not quite to the original level, due to the coexistence of a small but nonnegligible amount of two-oxygen coordinated Cu(I) ions. The higher shell structure also becomes clearly visible again, indicating a tight bonding of Cu(II) to the zeolite framework even at this temperature.

CH_4 versus C_3H_6 as a Reducing Agent. For comparison purposes, we studied the Cu(I) concentration change at different reaction temperatures in a $NO/CH_4/O_2/N_2$ = 2300vppm/5200vppm/5.3 vol %/balance mixture. XANES spectra at a few selected temperatures are plotted as the dashed lines in Figure 3 and the corresponding normalized difference XANES are shown in Figure 4c. In this study, the methane concentration was adjusted so that its ratio to NO and O_2 is stoichiometrically equivalent to that of propene in the previous study. Although it has been shown that methane is an effective reducing agent of NO over Co−ZSM-5,[24−26] it demonstrates no significant catalytic reduction selectivity for NO over Cu-ZSM-5,[27] presumably due to copper's lack of capability to activate the C−H bond of methane. Indeed, at the temperature for the optimum NO conversion by propene (ca. 625 K), XANES spectra show no significant Cu(I) transition intensity in the methane mixture. With a further increase of the temperature, a weak Cu(I) transition at 5.3 eV, which is also observed in the propene mixture as mentioned earlier, gradually increases its intensity. At $T = 873$ K, XANES spectra are basically identical in both cases. Using the same integration method, we calculated the Cu(I) transition intensity at various reaction temperatures and plotted them in Figure 3 as the solid squares. No window of Cu(I) enhancement is found over the same temperature range studied. Rather, we observed a monotonic, slowly increasing Cu(I) intensity with the increase of the reaction temperature.

Applying the same approach we used in SCR by propene, we also studied the copper ion coordination by in situ EXAFS method. Plotted in Figure 8a is the RDF of Cu in Cu-ZSM-5−

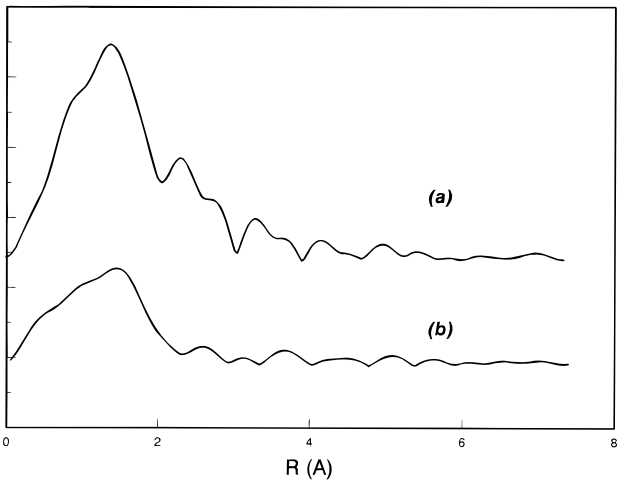

Figure 8. Radial distribution functions (RDF) of Cu in Cu-ZSM-5−150 obtained from Fourier transformation of the χ function of EXAFS spectra which were taken at $T = 625$ K in the reaction mixtures of (a) $NO/CH_4/O_2/N_2 = 2300$vppm/5200vppm/5.3 vol %/balance and (b) $NO/C_3H_6/O_2/N_2 = 3200$vppm/3200vppm/7.5 vol %/balance.

150 at T = 625 K in the $NO/CH_4/O_2/N_2$ mixture. For comparison, the RDF of Cu in the $NO/C_3H_6/O_2/N_2$ mixture at the same temperature is also plotted in Figure 8b. The spectral fitting of the inverse Fourier transformed EXAFS from Figure 8a confers that the first-shell coordination of the copper ion consists of approximately four oxygens with a shell radius of 1.93 Å, a further indication that Cu in Cu-ZSM-5 is mostly cupric saturated by oxygen, similar to its stable form at ambient temperature in air. Methane does not chemisorb on the surface of copper ion; therefore, it does not generate any significant reduction of cupric to cuprous ion in excess of oxygen at this temperature. With a further increase of the temperature, a small fraction of cuprous ions is gradually formed as result of autoreduction through oxygen desorption, in a similar fashion as that observed in the NO direct decomposition reaction.[19]

We should point out that although weak in reducing power, methane can still result in reduction of Cu(II) to Cu(I) in the absence of oxygen. We observed in our experiment that a significant amount of cuprous ion is formed in a 1% CH_4/N_2 mixture around 673 K.

C_3H_8 versus C_3H_6 as a Reducing Agent. Similar to propene, propane is also a selective reducing agent for NO conversion, albeit with less catalytic efficiency.[22] We studied the Cu(I) transition intensity as a function of reaction temperature in the same approach described above in a gas mixture where C_3H_6 is replaced by C_3H_8. A selected group of XANES spectra at corresponding temperatures is plotted as chain−dot lines in Figure 3, and their corresponding normalized difference XANES spectra are shown in Figure 4b. Interestingly, although at both low and high temperatures the XANES spectra are practically overlapping with those observed in the other two gas mixtures, the rest represent somewhat intermediate cases between that of methane and propene at the medium-temperature range. For example, at $T = 642$ K, the 1s → 4p transition of Cu(I) is clearly observed, although the intensity is significantly weaker than that observed in the propene mixture. The Cu(I) transition intensities calculated from the same method used in earlier discussions are plotted as solid triangles in Figure 5. A window of Cu(I) ion concentration enhancement is also observed for this SCR reaction. The intensities are significantly lower and the temperature span narrower than that in the case of propene. Both intensity and temperature variations seem consistent qualitatively with the catalytic performance of the propane mixture. In addition to the weak temperature window, a continually rising Cu(I) background with an increase in temperature is also observed, which overlaps with that observed in propene and methane mixtures.

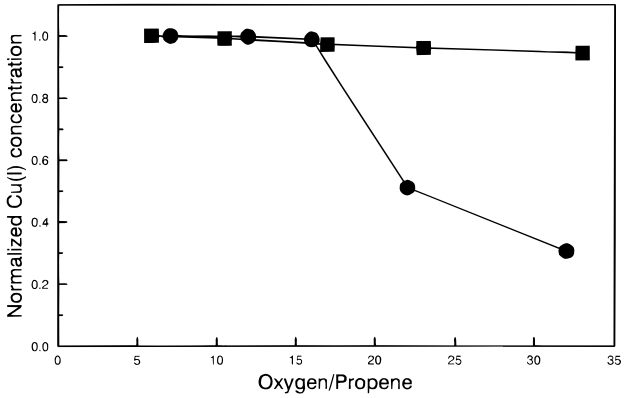

Figure 9. Dependence of the Cu(I) concentration on the oxygen-to-propene ratio, O_2/C_3H_6, for both under-exchanged Cu-ZSM-5−50 (●) and over-exchanged Cu-ZSM-5−150 (■).

Closer examination of the Cu(I) 1s → 4p transition indicates that it has similar characteristics to the cuprous species with higher peak energy (5.3 eV). The implication of this on the mechanism of NO SCR by propane will be discussed later.

Another important feature distinctively different in NO SCR−propane from that in SCR−propene is the color of Cu-ZSM-5 after an extended period of catalysis at optimum conversion temperature. As the catalyst's color remains white in a propane mixture, similar to its appearance after dehydration, it turns dark grayish or even black after a sustained period of operation in a propene mixture. This suggests that carbonaceous material formation over Cu-ZSM-5 is much less, if any, for propane than for propene.

Effect of Oxygen on Cu in Cu−ZSM-5. We found that during the selective reduction of NO by propene, the dependence of the cuprous ion concentration on the reaction temperature was insensitive to NO content, as long as O_2 is in excess. For example, we observed very similar temperature windows in the reaction mixtures of $NO/C_3H_6/O_2/N_2 = 1000$vppm/1000vppm/1 vol %/balance to that in the mixture of $C_3H_6/O_2/N_2 = 1000$vppm/1 vol %/balance. Although it is almost independent of the presence of NO, Cu(I) does depend on the oxygen content or more properly on the oxygen-to-propene ratio, O_2/C_3H_6. For instance, we investigated Cu(I) concentration as a function of O_2/C_3H_6 for both 50% exchanged and 150% exchanged Cu-ZSM-5 at their optimum NO conversion temperatures, 673 and 625 K, respectively. Shown in Figure 9 are the normalized Cu(I) concentrations measured at several oxygen/propene values. We found that while Cu(I) concentration decreases significantly with the increase of O_2/C_3H_6 for 50% exchanged Cu-ZSM-5, it drops only slightly for 150% exchanged Cu-ZSM-5. The slight decrease of Cu(I) concentration for 150% exchanged Cu-ZSM-5 also correlates qualitatively with the variation of NO conversion level versus oxygen measured by Iwamoto and co-workers,[3] as demonstrated in Figure 17 of ref 3.

The dependence of the Cu(I) content versus the oxygen/propane ratio was also studied for C-ZSM-5−150 in a $NO/C_3H_8/O_2/N_2$ mixture at 673 K. Plotted in Figure 10 are normalized cuprous ion concentrations at various O_2/C_3H_8 ratios where the Cu(I) ion content was assigned to unity at $O_2/C_3H_8 = 5$. Although the Cu(I) concentration decreases fast at the low oxygen-to-propane ratio, it becomes less sensitive at higher O_2/C_3H_8 values.

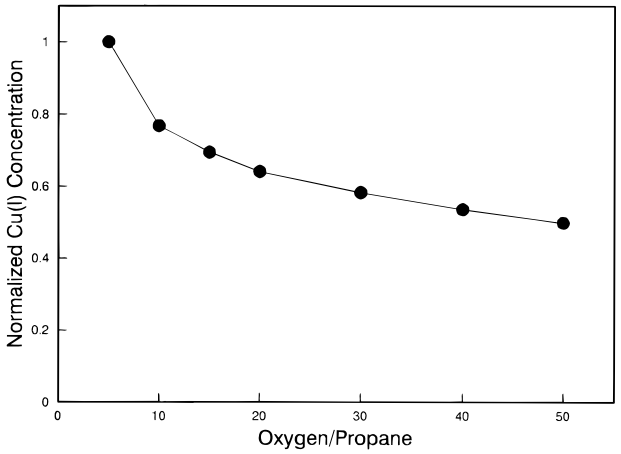

Figure 10. Dependence of the Cu(I) concentration on the oxygen-to-propane ratio, O_2/C_3H_8, for Cu-ZSM-5−150 at 673 K in a mixture of $NO/C_3H_8/O_2/N_2$.

By removing O_2 completely from the stream, we found that Cu ions in Cu-ZSM-5 are almost completely reduced to cuprous ions. Continuous reaction under this strongly reducing stream at elevated temperature will result in the formation of metallic copper.

Discussion

Our experimental results clearly demonstrate the presence of cuprous ions in ZSM-5 during the selective reduction of NO by propene and propane in excess oxygen. The variation of Cu-(I) concentration with temperature seems also to approximately correlate with the NO conversion rate. The existence of this correlation represents the key difference between the selective NO catalytic reduction and nonselective reaction, such as in the case of methane for the Cu-ZSM-5 system. These results favor a redox mechanism in which Cu(I) acts as an active intermediate for NO conversion. More details on the nature of the active site can be elaborated through analysis of the electronic transition and the local structure of the copper ions during the catalytic reaction.

The Nature of the Active Site. In the case of SCR by C_3H_6, cuprous ion transition intensity depends strongly on the presence of propene. It is quite certain that the substantial amount of Cu(I) ions formed between 500 and 700 K are through chemical reduction by propene. In fact, within the temperature span for the optimum selective reduction of NO by propene, the XANES spectral patterns appear quite differently from those we observed in a direct decomposition study (such as peak energy, spectral pattern, etc).[19,20] For example, a careful measurement of the transition energy in Figures 3 and 4 indicates that, at a temperature slightly higher than the onset of NO reduction by C_3H_6 (514 K), the center of the Cu(I) 1s → 4p transition is located at 4.1 eV above zero. To facilitate the following discussion, we name this transition as T_a and label its position with a chain−dash line in Figures 3 and 4. Increasing the reaction temperature from 500 to 650 K (within the "window"), the intensity of the Cu(I) transition increases and the center shifts gradually to a higher energy. At a temperature above 700 K (outside the window), the intensity decreases abruptly and the peak energy shifts to 5.3 eV with a much weaker intensity. A further increase of the temperature does *not* result in the continuous shift of the peak energy. This transition is located at the same energy as those we observed for Cu(I) in Cu-ZSM-5 during direct NO decomposition.[19,28] In that study, the intensity of the same peak increases with temperature without an energy shift, due to the autoreduction of Cu(II) through oxygen desorption. The spectral peak was assigned to the 1s → 4p transition of Cu(I) ion coordinated by two oxygen atoms.[19,20] We name this transition as T_b and label its position with another chain-dash line. Another transition at 7.5 eV, as shown in Figure 4, was assigned to 1s → 4p transition of Cu(II) ion.

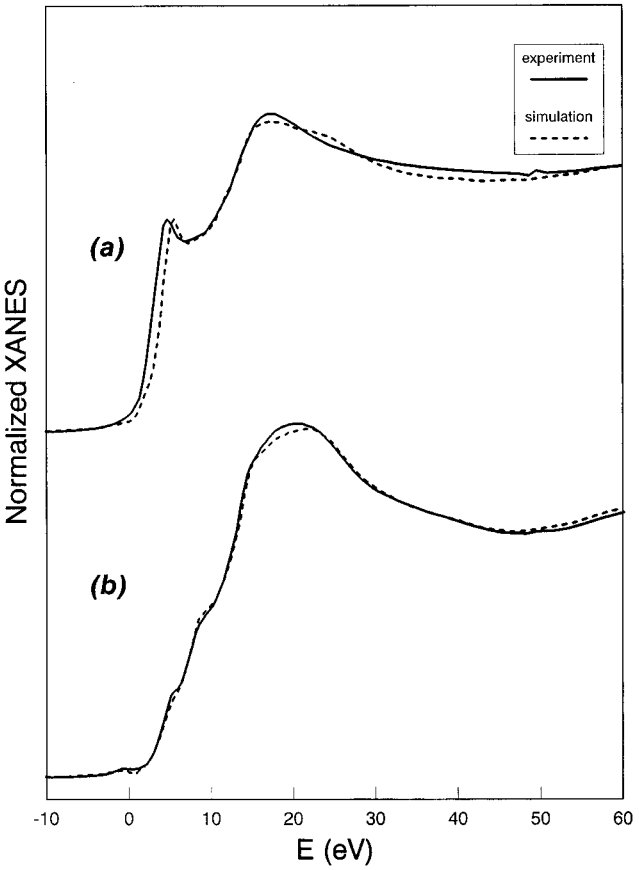

Figure 11. Experimental (—) and simulated (···) XANES spectra of Cu in Cu-ZSM-5 taken at $T = 642$ K in a (a) $NO/C_3H_6/O_2/N_2$ and (b) $NO/C_3H_8/O_2/N_2$ gas mixture.

In our earlier direct NO decomposition study, we established a good understanding of the structure and electronic properties of T_b. We identified that the cuprous ion associated with the transition T_b is the active species in a catalytic redox cycle.[19,20] Furthermore, we found that the Cu XANES spectrum under NO decomposition conditions at any given temperature can be reconstructed by a simple fractional summation of a pair of reference XANES spectra, one from a fully oxidized Cu(II)-ZSM-5 (zero T_b intensity) and the other from a fully autoreduced Cu(I)-ZSM-5 (full T_b intensity). Since each XANES spectrum is intensity-normalized, the contribution of each spectrum simply represents the fractional concentration of Cu(I) or Cu(II) in ZSM-5. Our EXAFS study also indicates that during the NO decomposition reaction, Cu(I) is coordinated by two O atoms at a Cu−O distance = 1.94 Å whereas Cu(II) is surrounded by four oxygens. Both types of ions are anchored at the zeolite exchange site through the migration at elevated temperatures.[19−21] During the catalytic redox cycle, the copper ions at the active site are switching between these two states. At any given temperature, the relative ratio of Cu(II)/Cu(I) varies in correlation with the rate of NO decomposition. However, no other Cu-(I) species was observed in that study.

We applied the same pair of reference spectra from the direct decomposition study to fit XANES spectra obtained during SCR NO by propene and propane. Shown in Figure 11 are two spectra

taken at $T = 642$ K for propene (Figure 11a) and propane (Figure 11b). The solid lines are the experimental XANES spectra, and the dotted lines are the simulation from the reference spectra. The fit between the experimental and the simulation spectra is quite good for Figure 11b. The fraction of Cu(I) calculated from this fitting is about 10%. The good fitting suggests that Cu(I) transition in SCR by propane is entirely from T_b. This is further confirmed by the difference XANES spectra in Figure 4b, where the Cu(I) peak energy remains unchanged even though the intensity varies with the temperature. The cuprous ions, though low in their content, are the same kind as that observed in the NO catalytic decomposition reaction. The low content is simply due to the suppression by excess O_2 in SCR. Therefore, no new cuprous species is formed. The experimental and simulation spectra in Figure 11a, however, do not match completely. The mismatch is not only observed in the Cu(I) 1s $\rightarrow$ 4p transition, which is anticipated due to a lower transition energy of T_a, but also in the entire XANES region 60 eV above the threshold. This suggests that the cuprous ions formed during SCR by propene, at least *a fraction of them*, are a new kind of Cu(I) intermediates different from that formed in direct NO decomposition. The mismatch also makes it difficult to quantify the exact amount of new Cu(I) species within the window of NO SCR by propene. Unless we could isolate the "pure" XANES spectrum attributed to T_a, we could not use the linear summation method to derive the fraction of new Cu(I) ions.

In X-ray absorption spectroscopy, the state-to-state transition energy depends strongly on electronic orbital interactions between the excited atom and its coordination environment. The cuprous 1s $\rightarrow$ 4p transition at 4.1 eV (T_a) observed at the onset of the selective reduction window suggests that the nature of this cuprous ion is different from that observed in NO decomposition (T_b). Rather, a new kind of cuprous ion is formed. The new Cu(I) formation likely involves two steps. First, the adsorption of propene by Cu(II) to form Cu(II)−propene. Then the reduction takes place through the intramolecular electron transfer to form a Cu(I)−alkene species. The lower transition energy of T_a suggests an electron transfer from the π orbital of the alkene intermediate to the *p* orbital of Cu(I), which results in a slight downshift of the Cu(I) 4p orbital energy. In fact, early studies of the Cu−Y zeolite system using UV and IR spectroscopies indicated that Cu(II) can be easily reduced to Cu(I) upon adsorption of propene to form a Cu(I) π-allylic intermediate,[29] although organometallic chemistry literature suggested that Cu(I) allylic compounds have a σ-bond nature.[30] The Cu(I) allylic intermediate can react quickly to remove two oxygen atoms to form an intermediate, Cu(I)−C_xH_y, with two oxygens coordinated. At present, we do not know the exact composition of C_xH_y experimentally other than to speculate that it can continue to grow with the presence of propene. A further increase of the catalytic temperature results in fast burnoff of the intermediate and direct reaction between propene and oxygen coordinated around Cu(II) without forming a quasi-stable allylic species. Therefore, a simple two-oxygen coordinated Cu(I) without a Cu−C bond (T_b type) is formed. Within the reaction window, both T_a and T_b types of cuprous ions coexist and the Cu(I) transition represents the superposition of the two. The T_b type becomes more dominant at higher temperatures as the result of gradual "burnoff" of the Cu−allylic bond. Consequently, we observe the gradual upshift of the Cu(I) peak energy toward T_b, as shown in Figures 3 and 4. Above the burnoff temperature of 700 K, only type T_b exists and the transition energy shift stops even though the intensity continues to increase. Propane, lacking a π bond, does not form the allylic intermediate. Only a small fraction of Cu(II) is converted to cuprous ion (T_b type) through the rapid reduction of the coordination oxygen with C_3H_8. Therefore, we only observed a T_b transition.

We should point out that we could not unambiguously confirm the Cu−C bond from our EXAFS data shown in Figure 6. As shown in Figure 6b, the first shell in the RDF function is relatively broad. The broadening could be result of another type of ligand at a similar bond distance and/or large amplitude thermal motion between weakly boned Cu(I)−O. Furthermore, carbon is a weak backscatterer which makes it difficult to detect. Although we provided the first-shell structure for Cu in Table 1, these parameters at $T = 625$ K represent only the average coordination number and bond distance of different types of Cu−O interactions. We believe that at least three types of Cu ions can coexist at NO SCR by propene at this temperature. They are (a) Cu(I) allylic complex with copper anchored by O^- in the zeolite framework, (b) Cu(I) coordinated by two oxygen, and (c) Cu(II) with four oxygens coordinated, respectively. At present, we cannot separate the contribution from any particular group among them in the Fourier-transformed EXAFS spectra.

At the temperature above the SCR window, only the T_b transition was observed in all cases. In fact, the fractional summation method can be applied under these circumstances, and the Cu(I) content calculated ranges from 5% to 15%, increasing with the increase of the temperature. At these temperatures, the hydrocarbons such as C_3H_6 and C_3H_8 oxidize quickly with oxygen at the external surface of the zeolite; therefore, it cannot reach the cupric ions inside the zeolitic channel effectively. The small amount of Cu(I) ions is formed mainly through the autoreduction through oxygen thermal desorption, albeit that the autoreduction is partially suppressed by the excess oxygen in the gas mixtures.

Mechanism of NO SCR by Hydrocarbons. The observation of the correlation between the Cu(I) formation and NO_x reduction activity reaffirmed the theory of the redox mechanism of NO SCR by hydrocarbons. To date, this mechanism has also been confirmed by many experimental studies mentioned earlier. This experimental observation on Cu-ZSM-5, however, should not be a surprise. Chemically speaking, all the transition-metal catalytic reactions involve a *reversible* electron transfer between the metal active site, reactant, and product through a complete reaction cycle. Therefore, all the catalytic reactions are redox reactions by definition. In most catalytic reactions, however, the transition states of the reaction intermediates are too short-lived or have too low a concentration to be monitored by any existing experimental method. In some cases, however, the concentrations of the transient intermediates, such as Cu(I) in Cu-ZSM-5, are high enough to be detected under the catalytic conditions.

On the basis of XANES and EXAFS analysis and the discussion on the nature of the active site, we have constructed the following redox reaction steps at different temperatures for the selective catalytic reduction of NO by propene:

(a) At the NO reduction threshold temperature (<420 K), an allylic intermediate is formed through the interaction of copper's d or p orbital with propene's π bond. Subsequently, 4-oxygen-coordinated cupric ion is reduced to 2-oxygen-coordinated cuprous ion with T_a transition. (To simplify, all the oxygen ligands of the copper ions are omitted from the following reaction equations. For example, Cu(II) is coordinated with 4 oxygens and Cu(I) is coordinated with 2 oxygens.)

$$Cu(II) + C_3H_6 \rightarrow Cu(II)-C_3H_6 \rightarrow Cu(I)-C_xH_y(T_a) \quad (1)$$

The cuprous ion is thus oxidized by NO and oxygen to finish the second half of the redox cycle.

$$Cu(I)-C_xH_y + NO + O_2 \rightarrow Cu(II) + N_2 + H_2O + CO_2 \quad (2)$$

(b) With the increase of the reaction temperature (420 K < T < 700 K), the reduction of Cu(II) to Cu(I) is gradually taken over by direct propene reduction to form type T_b cuprous ion with 2 oxygen coordination.

$$Cu(II) + C_3H_6 + O_2 \rightarrow Cu(I)(T_b) + H_2O + CO_2 \quad (3)$$

The reduction of NO follows this reaction

$$Cu(I) + NO \rightarrow Cu(I)-NO \rightarrow Cu(II) + N_2 + O_2 \quad (4)$$

In fact, in this temperature range, both reactions 1 and 3 coexist, as demonstrated by the coexistence of T_a and T_b transitions in XANES spectra. The balance shifted toward T_b at higher temperature. Direct reduction by propene (eq 3) gradually takes over.

(c) A further increase of the temperature (T > 700 K) turns Cu-ZSM-5 into an oxidation catalyst. The propene molecules burn quickly with oxygen on the external surface of Cu-ZSM-5 before reaching Cu(II) inside of the zeolite channel. Reduction by propene becomes less effective, and Cu(I) concentration decreases rapidly. At higher temperature, however, the autoreduction of Cu(II) to Cu(I) due to the desorption of oxygen becomes more facile. This follows the same redox reaction path observed in direct NO decomposition study[19,20]

$$Cu(II) \rightarrow Cu(I)(T_b) + O_2 \quad (5)$$

while the NO reduction reaction at the active site follows the same path as eq 4. At this temperature, the catalytic mechanism is basically the same as that of the direct NO decomposition reaction, except the rate is suppressed by the excess amount of oxygen in the mixture.

In the case of propane, we did not observe the formation of the allylic intermediate as given by eq 1. Rather, the reduction step of the redox cycle is accomplished similarly to eq 3 in the SCR window, i.e.,

$$Cu(II) + C_3H_8 + O_2 \rightarrow Cu(I)(T_b) + H_2O + CO_2 \quad (6)$$

and eq 4. At the temperature above the window, the catalytic mechanism is the same as that discussed in eq 5 and so forth.

Even though the catalytic activity of NO SCR by propane is less than that of NO SCR by propene, which seems to agree with the difference in Cu(I) intensities in Figure 5, one should not take this comparison quantitatively. In the case of propene, we believe that a significant amount of Cu(I) is trapped inside the zeolite channel by the carbonaceous material, which therefore becomes the spectator. This group of Cu(I) will participate in the catalysis only after the pore is reopened by removal of carbon deposit through the oxidation.

Methane is known to have the weakest reducing power among the hydrocarbons. Its symmetric structure (T_d) and high C−H bond activation energy make it difficult to be adsorbed and dissociated over the transition-metal surface. This appears to be the case in our Cu-ZSM-5 study. In the NO catalytic reduction in the presence of oxygen, we could not identify the conversion of Cu(II) to Cu(I) specifically due to CH_4 interaction. The monotonic yet slow increase of Cu(I) with the temperature is associated with the autoreduction through thermodesorption of oxygen, as described by eq 5. At lower temperature, methane does not adsorb and react with copper ions. At higher temperature (above the light-off temperature of methane combustion), methane reacts with oxygen at the external surface of the zeolite and forms CO_2 and H_2O.

Role of Oxygen in SCR. Although a variety of mechanisms involving oxygenated reaction intermediates, including nitro and nitrite species, have been proposed for SCR, we could not unambiguously confirm their existence in our EXAFS and XANES study. Our EXAFS analysis was not able to distinguish whether any of the first-shell oxygen is from the oxygenated intermediate. We believe that in addition to participating in the reactions in eqs 2, 3, and 6, one of the critical roles that oxygen plays in NO SCR is to balance the reducing and oxidizing environment to avoid the over-reduction by hydrocarbons, therefore to facilitate the redox reaction mechanism. Zeolites have a strong affinity toward the hydrocarbons. They interact with hydrocarbons easily and promote reaction with the transition-metal ions inside of the its channel. In the absence of oxygen, even methane can reduce Cu(II) to Cu(I), as reported earlier. The hydrocarbons such as propene and propane will reduce the metal ion continuously to its zero-valance state without sufficient oxygen. Furthermore, the excess hydrocarbons will isomerize and dehydrogenate in the zeolite and form carbonaceous deposits, which subsequently will block the zeolite channel and deactivate the catalytic reaction. This is particularly true in the case of NO SCR by propene.

Influence of the Carbonaceous Deposit. A frequently debated issue in the selective NO reduction catalytic mechanism is the role of the carbonaceous materials deposited during the reaction. It has been shown that a precoked Cu-ZSM-5 momentarily retains its activity for NO conversion in the absence of C_3H_6, and the activity is significantly enhanced by the presence of oxygen.[6,10] These observations led to the proposal that one of the key intermediates of the reaction is the coke, and the role of oxygen is to form a $Cu-NO_2$ species.[10] Others suggested that the carbonaceous deposit acts as a reservoir of reducing agent to maintain the copper in the optimum oxidation state in the presence of oxygen.[6]

We investigated this problem by switching the reactant stream from air to the NO/propene/O_2/N_2 = 3200vppm/3200vppm/7.5 vol %/balance mixture at 673 K and subjecting the Cu-ZSM-5 for an extended period (about 1 h or more) of catalysis. Indeed, we observed that the catalyst turned dark gray, indicating the build-up of carbonaceous deposit. XANES spectra showed that Cu(I) reached a steady-state concentration quickly (in about 10 min). By switching off propene in the stream, Cu(I) is reoxidized to Cu(II) in a few minutes and the color of the catalyst turns to off-white. This observation supports a link between cuprous ion formation and carbonaceous material build-up. We suspect that some of the build-up is through the last step in eq 1 where Cu(I)$\cdots C_xH_y$ continues to react with more propene at elevated temperature, although it is also commonly believed that the carbonaceous formation is caused by a residual proton in the zeolite. Some of this carbon deposit can block the zeolitic channels. The build-up will eventually stop due to the balancing process of oxidation. When the propene is switched off, NO will be continuously catalyzed by the available Cu(I) site. The oxygen and NO in the stream will also un-plug the coked zeolite channels and expose additional Cu(I) sites until all the cuprous ions are reoxidized to cupric ions and catalytic activity stops.

The carbonaceous deposit was much less in NO SCR by

TABLE 2: Difference and Similarity in the Oxidation State, Coordination Structure, and Reaction Mechanism between NO Decomposition and NO SCR by Hydrocarbons over Cu-ZSM-5

NO decomposition	NO SCR by hydrocarbons
The cuprous ion, Cu(I), is observed during the direct NO catalytic decomposition, suggesting a redox mechanism in which the catalyst's active site is Cu(I). Cu(I) is formed through the autoreduction at elevated temperature, which probably involves an oxygen desorption process through a dicopper intermediate. Cu(I) formation is sensitive to the Cu exchange level, and the "excessively" exchanged Cu-ZSM-5 maintains a higher concentration of Cu(I) than that of "underexchanged" under the reaction conditions.	The cuprous ion is also observed during the NO selective catalytic reduction by hydrocarbons, suggesting a redox mechanism which involves the conversion between Cu(II) and Cu(I). Cu(I) is formed through the reduction by hydrocarbons. The rate of formation of Cu(I) is not sensitive to the exchange level, rather it is very sensitive to the type of hydrocarbons used. The reducing power is $C_3H_6 > C_3H_8 > CH_4$ with methane practically equal to zero.
The 1s $\rightarrow$ 4p electronic transition of Cu(I) does not shift its energy at different reaction temperatures, indicating that no change of the Cu(I) environment and catalytic pathway occurs.	The 1s $\rightarrow$ 4p transition energy shifts at different reaction temperatures in NO SCR with propene, indicating that the Cu(I) local coordination varies, which corresponds to different redox pathways. No energy shift is observed in a propane or methane mixture.
The cuprous ion formed through autoreduction is coordinated by two oxygen atoms. No clear higher shell structure is observed. Under direct NO decomposition, copper ions consist of a mixture of Cu(I) and Cu(II), Cu(II) is coordinated by four oxygen atoms.	Cu(I) formed by olefin (propene) reduction is also coordinated by two oxygen atoms, with a possible Cu allylic bond which was not identified unambiguously. No evidence of the allylic compound formation was observed for propane and methane mixtures.
Cu(I) concentration increases with the reaction temperature and is correlated with the NO decomposition rate from 300 to 500 °C. The discrepancy in correlation observed at higher temperature was attributed to slower migration/adsorption of NO to the active site inside of the zeolitic channel due to strong thermal vibration/distortion of the channel structure.	Cu(I) concentration as a function of the reaction temperature depends on the gas compositions. For SCR by propene, normalized Cu(I) intensity at various temperature appears to overlap with the normalized reaction rate versus the temperature. A similar correlation was also observed for SCR by propane. At higher temperature, the external oxidation of hydrocarbons dominates and NO SCR diminishes.
Cu(I) concentration decreases rapidly with the increase of the oxygen concentration in the gas phase, so does the NO decomposition activity.	The Cu(I) concentration decreases gradually with the increase of the oxygen concentration. In addition to participating reactions, the excess O_2 helps to balance the reducing/oxidizing environment and minimize the "coking".

propane and was not observed when propene or propane was replaced by methane.

Impact of Zeolitic Structure on Cu Redox Behavior. The zeolitic structure has a strong impact on the redox behavior of the exchanged copper ion. To verify this, we conducted an in situ XAS study in the same $NO/C_3H_6/O_2/N_2$ mixture except that Cu-ZSM-5 was replaced by highly dispersed CuO over SiO_2 with comparable Cu loading. Contrary to the case of Cu-ZSM-5, only a very small amount of Cu(II) converted to Cu(I) at the elevated temperature. This observation suggests that Cu ions exposed at the outer surface of the support are much less likely to convert to the cuprous form, which may be the cause of the lower NO reduction activity over CuO/SiO_2.

Almost all the copper-exchanged zeolites exhibit a certain degree of NO SCR activity, although the catalytic rate varies significantly between different types of zeolite. This is supported by ample amount of experimental evidence for copper or other transition-metal-exchanged zeolites.[2−19,24−27] It would be interesting to investigate whether different zeolites could also result in different Cu redox behavior, so that a simple correlation can be found for the sake of catalyst design. To this approach we studied another copper-exchanged zeolite with a much lower SCR activity under similar reaction conditions. A similar temperature window of Cu(I) formation, both in magnitude and width, was also observed even though the catalytic activity was significantly less. This experiment demonstrates that Cu(I) enhancement in Cu-ZSM-5 is far from unique among the copper-exchanged zeolites. The observation appears to contradict the redox mechanism but in fact it does not. In NO SCR, the zeolitic framework provides a suitable environment for maintaining a reasonably high level of cuprous ion in a strong oxidative condition. This electronic property alone, however, cannot account for the entire mechanism of NO reduction. Cuprous ions as active sites only provide the necessary prerequisite for the redox reaction. The zeolitic structure, which defines the exchange site location and its accessibility to the reactants such as NO, hydrocarbon, O_2, and water during the diffusion process, will also determine the efficiency of the overall reaction. Probing the change of the transition-metal oxidation state alone cannot resolve the sensitivity of the NO reduction rate due to the zeolitic structure. More experiments and theoretical simulations focusing on the structural dependent behavior, such as competition of migration of NO versus other oxidizing species in the ZSM-5, will shed light on the overall picture of NO SCR.

Comparison between Direct NO Decomposition and NO SCR by Hydrocarbons. From this study of NO SCR by hydrocarbons and our earlier investigation on NO decomposition over Cu-ZSM-5 catalyst, we summarize the mechanistic similarity and difference between the two catalytic reactions in Table 2.

Summary

We presented a detailed description of our experimental approach of using in situ X-ray absorption techniques to study the physical properties of copper in Cu-ZSM-5 during the selective catalytic reduction of NO by hydrocarbons. We also discussed our analysis of the nature of the active sites and the mechanism of the NO SCR based on the copper electronic and coordination structures derived from the experimental data. Our results demonstrated a cyclic redox mechanism involving Cu(I) and Cu(II) in an oxygen-rich gas mixture under elevated temperatures. An approximate correlation between cuprous ion concentrations and catalytic activities was found in NO SCR by propene and propane. The type of hydrocarbons in the gas mixture clearly influences the formation of the reaction intermediates and their redox behaviors during the catalysis. The impact of excess oxygen and the carbonaceous material on the catalytic reaction pathways is discussed. We also compiled the similarity and difference in the reaction mechanism and the physical properties of copper ion between NO catalytic decomposition and NO SCR.

Acknowledgment. We thank Dr. Karl C. C. Kharas for providing the samples and Mr. Mike A. Reddig for technical assistance. Financial support of AlliedSignal Inc. is gratefully acknowledged. Research was carried out (in part) at Beamline X-18B of the National Synchrotron Light Source, Brookhaven National Laboratory, which is supported by the U.S. Department

of Energy, Division of Materials Sciences and Division of Chemical Sciences.

References and Notes

(1) Held W.; Koenig, A.; Richter, T.; Puppe, L. SAE Paper 900496, 1990.

(2) Iwamoto, M.; Yahiro, H.; Shundo, S.; Yu-u, Y.; Mizuno, N. *Shokubai* 1990, *33*, 430.

(3) Iwamoto, M.; Mizuno, N.; Yahiro, H. *Sekiyu Gakkaishi* **1991**, *34*, 375.

(4) Li, Y.; Hall, W. K. *J. Catal.* **1991**, *129*, 202.

(5) Valyon, J.; Hall, W. K. *J. Phys. Chem.* **1993**, *97*, 1204.

(6) Burch, R.; Millington, P. J. *Appl. Catal. B* **1993**, *2*, 101.

(7) Montreuil, C. N.; Shelef, M. *Appl. Catal. B* **1992**, *1*, L1.

(8) Inui, T.; Iwamoto, S.; Kojo, S.; Yoshida, T. *Catal. Lett.* **1992**, *13*, 87.

(9) Yamashita, H.; Yamada, H.; Tomita, A. *Appl. Catal.* **1991**, *78*, L1.

(10) Ansell, G. P.; Diwell, A. F.; Golumski, S. E.; Hayes, J. W.; Rajaram, R. R.; Truex, T. J.; Walker, A. P. *Appl. Catal. B* **1993**, *2*, 81.

(11) Petunchi, J. O.; Hall, W. K. *Appl. Catal. B* **1993**, *2*, L17.

(12) Petunchi, J. O.; Sill, G.; Hall, W. K. *Appl. Catal. B* **1993**, *2*, 303.

(13) Blint, R. J. *J. Phys. Chem.* **1996**, *100*, 19518.

(14) Yan, J. Y.; Sachtler, W. M. H.; Kung, H. H. *Catal. Today* **1997**, *33*, 279. Adelman, B. J.; Beutel, T.; Lei, G.- D.; Sachtler, W. M. H. *Appl. Catal. B* **1996**, *11*, L1. Beutel, T.; Sarkany, J.; Lei, G.-D.; Yan, J. Y.; Sachtler, W. M. H. *J. Phys. Chem.* **1996**, *100*, 845.

(15) Centi, G.; Galli, A.; Perathoner, S. *J. Chem. Soc., Faraday Trans.* **1996**, *92*, 5219.

(16) Rodriguez-Santiago, L.; Sierka, M.; Branchadell, V.; Sodupe, M.; Sauer, J. *J. Am. Chem. Soc.* **1998**, *120*, 1545.

(17) Brand, H. V.; Redondo, A.; Hay, P. J. *J. Phys. Chem. B* **1997**, *101*, 7691.

(18) Shelef, M. *Chem. Rev.* **1995**, *95*, 209.

(19) Liu, D.-J.; Robota, H. J. *Catal. Lett.* **1993**, *21*, 291.

(20) Liu, D.-J.; Robota, H. J. *Reduction of Nitrogen Oxide Emissions*; Ozkan,U. S., Agarwal, S. K., Marcelin, G., Eds.; ACS Symposium Series 587; American Chemical Society: Washington, DC; Chapter 12, p 147.

(21) Liu, D.-J.; Robota, H. J. *Appl. Catal. B* **1994**, *4*, 155.

(22) Kharas, K. C. C. *Appl. Catal B* **1993**, *2*, 207.

(23) Kau, L.-S.; Spira-Solomon, D. J.; Penner-Hahn, J. E.; Hodgson, K. O.; Solomon, E. I. *J. Am. Chem. Soc.* **1987**, *109*, 6433.

(24) Li, Y.; Armor, J. N. U.S. Pat. 5 149 512, 1992.

(25) Li, Y.; Armor, J. N. *Appl. Catal. B* **1992**, *1*, L31.

(26) Cowan, A. D.; Dümpelmann, R.; Cant, N. W. *J. Catal.* **1995**, *151*, 365.

(27) Iwamoto, M.; Mizuno, N.; Yahiro, H. *Stud. Surf. Sci. Catal.* **1993**, *75*, 1285.

(28) Our earlier report, ref 19, of this energy measurement was 4 eV. Our new energy calibration shows that the transition is located about 5.3 eV above the first inflection point in the Cu(0) fluorescence excitation spectrum, with an estimated uncertainty of ±0.3 eV. We also observed that the Cu(0) edge appears at about 1 eV to higher energy in the transmission spectrum than that observed in the fluorescence excitation spectrum.

(29) Coudurier, G.; Decamp, T.; Praliaud, H. *J. Chem. Soc., Faraday Trans.* **1982**, *78*, 2661.

(30) Yamamoto, Y.; Asao, N. *Chem. Rev.* **1993**, *93*, 2207.